ELSEVIER

Journal of Organometallic Chemistry 573 (1999) 254–260

Journal of Organo metallic Chemistry

Solid state studies (X-ray and ^{1}H-, ^{13}C-NMR) on $(NMe_4)_{4-x}[H_xNi_{12}(CO)_{21}] \cdot S$ ($x = 1$, $S = Me_2CO$; $x = 2$, $S = 2THF$)[1]

James V. Barkley [a], Taro Eguchi [b,*], Rachel A. Harding [b], Brian T. Heaton [a],
Giuliano Longoni [c], Lucia Manzi [a], Hirokazu Nakayama [2,b], Kei Miyagi [b],
Anthony K. Smith [3,a], Alexander Steiner [a]

[a] *Department of Chemistry, University of Liverpool, Liverpool L69 7ZD, UK*
[b] *Department of Chemistry, Graduate School of Science, Osaka University, Toyonaka, Osaka 560-0043, Japan*
[c] *Dipartimento di Chimica Fisica ed Inorganica, Universit di Bologna, Viale Risorgimento 4, 40136 Bologna, Italy*

Received 16 April 1998

Abstract

The molecular structures of $(NMe_4)_{4-x}[H_xNi_{12}(CO)_{21}] \cdot S$ ($x = 1$, $S = Me_2CO$; $x = 2$, $S = 2THF$) are reported. Both anions are similar and consist of a central $Ni_6(CO)_3(\mu\text{-}CO)_6$-layer flanked on both sides by two $Ni_3(CO)_3(\mu\text{-}CO)_3$-layers such that the Ni_{12}-fragment is hexagonal close-packed. The separation between the central Ni_6-plane (B) and the two outer Ni_3-planes (A, C) is consistent with H-occupancy of either one ($x = 1$) or both ($x = 2$) of the two octahedral metal cavities. Variable temperature solid state ^{1}H MAS and ^{13}C CP/MAS NMR spectra are reported for both clusters. For the dihydride, the solid state ^{1}H- and ^{13}C-NMR spectra remain unchanged from low to room temperature and are consistent with the X-ray structure; at room temperature, there are two hydride resonances consistent with them being on the plane of symmetry on opposite sides of the Ni_6-layer and the highfield shift is consistent with them not being in the centre of the Ni_6 octahedral cavity. For $[H_2Ni_{12}(CO)_{21}]^{2-}$, there is close agreement between the solution and solid state ^{13}CO chemical shifts except for the inner bridging carbonyls which appear in solution as one resonance whereas in the solid state occur as two resonances due to the bridging CO's being either above or below the Ni_6-plane. At higher temperatures, there is evidence for H movement (probably oscillation about the plane of symmetry) but ^{13}C spectra indicate that the CO's remain essentially static. For the monohydride, three of the bridging CO's are almost co-planar with the Ni_6-plane, one, C6, is significantly bent towards the hydride and two CO's are in intermediate positions; the low temperature solid state ^{13}CO-NMR spectra appear to be entirely consistent with this structure. At room temperature, there is some coalescence of the ^{13}CO resonances, suggesting some carbonyl movement, but there is no evidence for H-migration from the occupied interstitial octahedral site to the unoccupied octahedral site.

Keywords: Nickel carbonyl clusters; X-ray structures; ^{1}H and ^{13}C solid state NMR; Interstitial hydride; Dynamics in solid state

---

1. Introduction

As part of our on-going comparative solution and solid state NMR study of hydrido transition metal carbonyl clusters [1], we now report the X-ray structures and ^{1}H MAS and ^{13}C CP/MAS solid state NMR spectra of $(NMe_4)_{4-x}[H_xNi_{12}(CO)_{21}] \cdot S$ ($x = 1$, $S = Me_2CO$; $x = 2$, $S = 2THF$)[4]. The tetramethylammonium salts were chosen because our previous work showed that there is efficient ^{1}H to ^{13}CO cross polarisa-

---

* Corresponding author. Fax: +44 151 7943540; e-mail: AMF@Liverpool.ac.uk

[1] Dedicated to Professor B.F.G. Johnson FRS, on the occasion of his 60th birthday for his outstanding contributions to inorganic chemistry, particularly cluster chemistry.

[2] Kobe Pharmaceutical University, Kobe, Japan.

[3] CPE, Lyon, France.

[4] It has proved impossible to remove the solvent of crystallisation associated with both clusters by heating and, throughout this paper, structures and measurements were carried out on these salts, although the solvent may not be specifically referred to.

PII S0022-328X(98)00766-9

Table 1

	$[HNi_{12}(CO)_{21}]^{3-}$		$[H_2Ni_{12}(CO)_{21}]^{2-}$	
Average distance (Å)	$(AsPh_4)^+$[3]	$(NMe_4)^+$	$(AsPh_4)^+$[3]	$(NMe_4)^+$
Interplanar, Ni_A–Ni_B distance[a]	2.382	2.366	2.442[c]	2.422[c]
Interplanar, Ni_B–Ni_C distance[a]	2.439[c]	2.408[c]	2.424[c]	2.409[c]
Dihedral angle[b], A–B, B–C	1.52, 1.48	0.6, 0.5	1.02, 0.43	0.2, 0.5
Distortion of the μ-CO's from the Ni_6-plane (B)		C(4) +0.032, C(5) +0.067, C(6) +0.143, C(7) −0.010, C(8) −0.012, C(9) −0.016,		C(1) −0.244, C(2) +0.228, C(3) −0.175, C(1)* −0.244, C(2)* +0.228, C(3)* −0.175

[a] Ni_6-plane = Ni_B, outer Ni_3-plane = Ni_A or Ni_C (for $x = 1$, Ni_A = Ni7, Ni8, Ni9; Ni_C = Ni10, Ni11, Ni12), with respect to centres of triangular Ni_{13}-moieties.

[b] Between outer Ni_3-plane (A, C) and central Ni_6-plane (B).

[c] Containing interstitial H.

tion transfer allowing excellent signal-to-noise ^{13}C CP/MAS NMR spectra to be obtained at natural ^{13}CO abundance levels [2]; additionally, because of the presence of fewer and sharper spinning side-bands, it was possible to obtain better quality solid state ^1H-NMR spectra than for the $(NEt_4)^+$ salts which had been used previously [1].

The structures of $(AsPh_4)_3[HNi_{12}(CO)_{21}]$ and $(PPh_4)_2[H_2Ni_{12}(CO)_{21}]$ have been previously established by both X-ray and neutron diffraction and the structures of $(PPN)_2[H_2Ni_{12}(CO)_{21}]$ and $(AsPh_4)_2[H_2Ni_{12}(CO)_{21}]$ have also been determined by X-ray crystallography [3]; the structure of the $(NMe_4)^+$ salt of the parent cluster $[Ni_{12}(CO)_{21}]^{4-}$ has also been determined [4] but none of these structures have been published in full. However, they have been variously alluded to as a result of other measurements [1], [5–8]. The overall structure of the anions in all the above cases and the $(NMe_4)^+$ salts described below are essentially the same, apart from distortions, with the hydride(s) occupying either one or both of the two octahedral metal cavities; in both the mono- and di-hydrides, neutron diffraction data show that the hydride is significantly displaced towards the central Ni_3-triangle and this is entirely consistent with our solid state ^1H-NMR data.

We now report the X-ray structures of $(NMe_4)_{4-x}[H_xNi_{12}(CO)_{21}] \cdot S$ ($x = 1$, $S = Me_2CO$; $x = 2$, $S = 2THF$) and their solid state ^1H MAS and ^{13}C CP/MAS variable temperature (VT) NMR spectra, which at $\leq$ 298 K are entirely consistent with the distortion found in their solid state structures; at higher temperatures, solid state NMR measurements provide important information about H- and/or CO-mobility.

2. X-ray structures of $(NMe_4)_{4-x}[H_xNi_{12}(CO)_{21}] \cdot S$ ($x = 1$, $S = Me_2CO$; $x = 2$, $S = 2THF$)

The structures of the mono- and di-hydride anions are based on the same motif which consists of a central $Ni_6(CO)_3(\mu\text{-}CO)_6$-layer flanked on each side by two $Ni_3(CO)_3(\mu\text{-}CO)_3$-layers. This gives rise to a Ni_{12}-fragment which is hexagonal close-packed containing two octahedral and six tetrahedral metal cavities. There are no bridging CO's between the central Ni_6- and outer Ni_3-layers.

Apart from distortions caused by packing effects induced by the different cations, the overall structures of these anions are similar to those determined previously for different cations. Neutron diffraction studies on $(AsPh_4)_3[HNi_{12}(CO)_{21}]$ and $(PPh_4)_2[H_2Ni_{12}(CO)_{21}]$ show that the hydride occupies an interstitial site in one or both of the metal octahedral cavities [3]. The hydrides are not in the centre of the octahedral cavity but are displaced towards the central layer and the presence of a hydride results in an associated expansion of the nickel-interplanar spacing (see Table 1); a similar expansion of the interplanar spacings is found for the $(NMe_4)^+$ salts (see Table 1) and this, together with the similarity of the values of $\delta(H)$ for the hydride(s) in solution using different cations, suggests that the hydride site occupancy in $[H_xNi_{12}(CO)_{21}]^{(4-x)-}$ ($x = 1, 2$) is essentially cation independent, since we have shown previously that the value of $\delta(H)$ for interstitial hydrides is very sensitive to the displacement of the hydride from the centre of the octahedral metal cavity [1].

Fig. 1 and Fig. 2 show the structures of the anions of $(NMe_4)_{4-x}[H_xNi_{12}(CO)_{21}] \cdot S$ ($x = 1$, $S = Me_2CO$; $x = 2$, $S = 2THF$) together with the numbering scheme and selected bond distances and angles are shown in Table 2 and Table 3.

For $(NMe_4)_2[H_2Ni_{12}(CO)_{21}]$, there is a plane of symmetry which is indicated in the numbering scheme in Fig. 1. The three Ni-layers (A, B, C)[5] are almost parallel (see Table 1) and the six nickel atoms in the inner Ni_6-layer (B) are virtually coplanar. However, whereas the terminal CO's on the inner layer (T_i) are

---

[5] Ni_A = Ni7, Ni8; Ni_B = Ni1, Ni2, Ni3, Ni4, Ni_C = Ni5, Ni6.

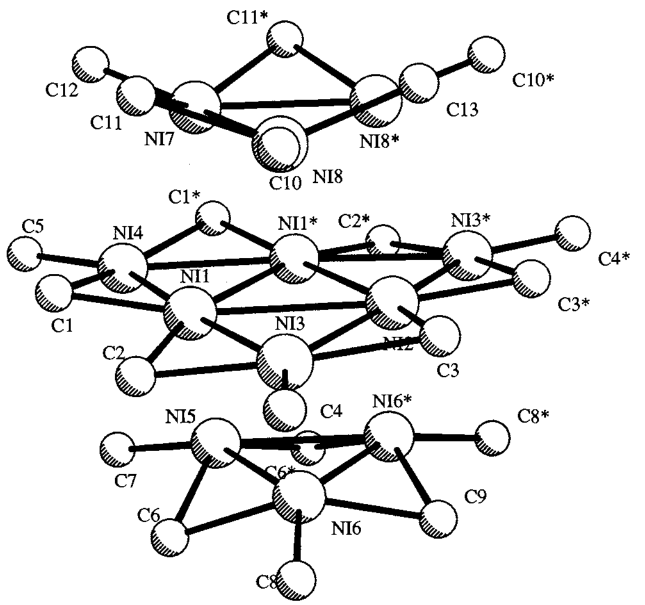

Fig. 1. Schematic representation of the X-ray structure of the anion in $(NMe_4)_2[H_2Ni_{12}(CO)_{21}] \cdot (2THF)$ and its numbering scheme.

Table 2

Selected comparative bond lengths (Å) for $(NMe_4)_2[H_2Ni_{12}(CO)_{21}] \cdot (2THF)$ and $(NMe_4)_3[HNi_{12}(CO)_{21}] \cdot Me_2CO$

$[H_2Ni_{12}(CO)_{21}]^{2-}$			$[HNi_{12}(CO)_{21}]^{3-a}$		
Ni(1)	Ni(1)*	2.639(3)	Ni(4)	Ni(5)	2.695(2)
Ni(1)	Ni(2)	2.658(3)	Ni(4)	Ni(6)	2.701(2)
Ni(1)	Ni(3)	2.421(3)	Ni(4)	Ni(1)	2.424(2)
Ni(1)	Ni(4)	2.412(3)	Ni(4)	Ni(2)	2.421(2)
Ni(1)*	Ni(2)	2.658(3)	Ni(5)	Ni(6)	2.687(2)
Ni(2)	Ni(3)	2.442(2)	Ni(5)	Ni(2)	2.420(2)
Ni(2)	Ni(3)*	2.442(2)	Ni(6)	Ni(1)	2.420(2)
Ni(3)*	Ni(1)*	2.421(3)	Ni(6)	Ni(3)	2.432(2)
Ni(5)	Ni(6)	2.431(3)	Ni(3)	Ni(5)	2.419(2)
Ni(5)	Ni(6)*	2.431(3)	Ni(11)	Ni(10)	2.435(2)
Ni(6)	Ni(6)*	2.448(3)	Ni(11)	Ni(12)	2.449(2)
Ni(7)	Ni(8)	2.431(3)	Ni(10)	Ni(12)	2.436(2)
Ni(7)	Ni(8)*	2.431(3)	Ni(8)	Ni(7)	2.420(2)
Ni(8)	Ni(8)*	2.426(3)	Ni(7)	Ni(9)	2.427(2)
Ni(1)	C(1)	1.88(1)	Ni(4)	C(5)	1.88(1)
Ni(1)	C(2)	1.89(1)	Ni(4)	C(4)	1.85(1)
Ni(2)	C(3)*	1.89(1)	Ni(6)	C(8)	1.86(1)
Ni(3)	C(2)	1.91(1)	Ni(1)	C(4)	1.90(1)
Ni(3)	C(3)	1.93(1)	Ni(1)	C(9)	1.91(1)
Ni(4)	C(1)	1.94(1)	Ni(2)	C(5)	1.89(1)
Ni(4)	C(1)*	1.94(1)	Ni(2)	C(6)	1.92(1)
Ni(5)	C(6)	1.92(1)	Ni(11)	C(21)	1.91(1)
Ni(5)	C(6)*	1.92(1)	Ni(11)	C(21)	1.91(1)
Ni(6)	C(6)	1.91(1)	Ni(10)	C(20)	1.89(1)
Ni(6)	C(9)	1.95(2)	Ni(10)	C(19)	1.89(1)
Ni(7)	C(11)	1.94(1)	Ni(8)	C(13)	1.92(1)
Ni(7)	C(11)*	1.94(1)	Ni(8)	C(14)	1.91(1)
Ni(8)*	C(11)*	1.95(1)	Ni(9)	C(14)	1.90(1)
Ni(8)*	C(13)	1.94(2)	Ni(9)	C(15)	1.91(1)

[a] The lack of symmetry for $[HNi_{12}(CO)_{21}]^{3-}$ imposes a different numbering scheme to that adopted by $[H_2Ni_{12}(CO)_{21}]^{2-}$ but the data are presented so that there is a direct comparison horizontally.

coplanar with the Ni_6-plane, four of the inner bridging CO's (B_i) are significantly bent up and the remaining two inner bridging CO's (C2, C2*) are bent down from the Ni_6 plane (see Table 1). There is a significant elongation of both Ni_A–Ni_B and Ni_B–Ni_C interplanar spacings consistent with hydride occupancy of each of the octahedral cavities on the plane of symmetry (see Table 1). All the CO-bridged Ni–Ni distances, both in the inner (2.425 Å) and outer (2.4305 Å) layers are similar and significantly shorter than the non CO-bridged Ni–Ni distances (2.658 Å) on the inner layer.

For $(NMe_4)_3[HNi_{12}(CO)_{21}]$, the structure of the anion is similar to that of the dihydride except that: (a) there is only one elongated interplanar Ni–Ni distance caused by the presence of one interstitial hydride (see Table 1), (b) there is no symmetry as indicated by the numbering scheme in Fig. 2. Nevertheless, for the inner bridging carbonyls, B_i, only one CO (C6) is significantly bent out of the Ni_6-plane towards the hydride with C7, C8 and C9 being almost coplanar with the Ni_6-plane and C4 and C5 are at intermediate positions (see Table 1).

As for the dihydride, the anion in $(NMe_4)_3[HNi_{12}(CO)_{21}]$ shows a similar variation in Ni–Ni distances. Thus, the CO-bridged Ni–Ni distances in the outer and inner plane are significantly (> 0.2 Å) shorter than the non CO-bridged Ni–Ni distances in the inner plane (see Table 2).

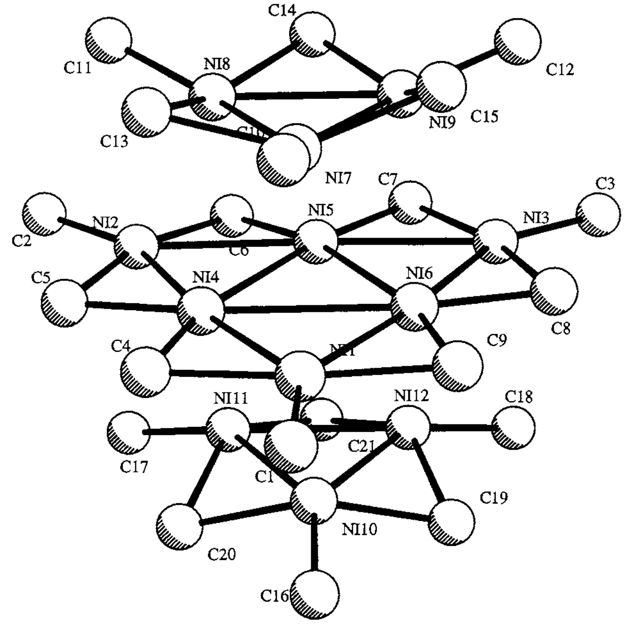

Fig. 2. Schematic representation of the X-ray structure of the anion in $(NMe_4)_3[HNi_{12}(CO)_{21}] \cdot Me_2CO$ and its numbering scheme.

Table 3
Selected comparative bond angles (°) for $(NMe_4)_3[HNi_{12}(CO)_{21}] \cdot Me_2CO$ and $(NMe_4)_2[H_2Ni_{12}(CO)_{21}] \cdot (2THF)$

$[H_2Ni_{12}(CO)_{21}]^{2-}$				$[HNi_{12}(CO)_{21}]^{3-}$[a]			
Ni(1)	Ni(1)*	Ni(2)	60.23(4)	Ni(4)	Ni(5)	Ni(6)	60.24(5)
Ni(1)*	Ni(1)	Ni(4)	56.82(5)	Ni(5)	Ni(4)	Ni(2)	56.16(5)
Ni(1)*	Ni(2)	Ni(3)*	56.48(6)	Ni(5)	Ni(4)	Ni(3)	56.14(5)
Ni(1)	Ni(3)	Ni(2)	66.28(8)	Ni(4)	Ni(1)	Ni(6)	67.80(6)
Ni(3)	Ni(1)	Ni(4)	174.26(9)	Ni(1)	Ni(4)	Ni(2)	171.91(6)
Ni(4)	Ni(1)*	Ni(3)	174.26(9)	Ni(2)	Ni(5)	Ni(3)	172.91(6)
Ni(3)*	Ni(2)	Ni(3)	172.0(1)	Ni(3)	Ni(6)	Ni(1)	172.33(7)
Ni(1)	C(1)	Ni(4)	78.1(5)	Ni(4)	C(5)	Ni(2)	79.9(4)
Ni(4)	C(1)*	Ni(1)*	78.1(5)	Ni(2)	C(6)	Ni(5)	79.2(4)
Ni(1)*	C(2)*	Ni(3)*	79.0(5)	Ni(5)	C(7)	Ni(3)	79.9(4)
Ni(3)*	C(3)*	Ni(2)	79.5(5)	Ni(6)	C(9)	Ni(1)	80.0(4)
Ni(3)	C(2)	Ni(1)	79.0(5)	Ni(1)	C(4)	Ni(4)	79.8(4)

[a] The lack of symmetry for $[HNi_{12}(CO)_{21}]^{3-}$ imposes a different numbering scheme to that adopted by $[H_2Ni_{12}(CO)_{21}]^{2-}$ but the data are presented so that there is a direct comparison horizontally.

3. Solid state NMR spectra of $(NMe_4)_{4-x}[H_xNi_{12}(CO)_{21}] \cdot S$ ($x = 1$, $S = Me_2CO$; $x = 2$, $S = 2THF$)

The room temperature (r.t.), natural abundance ^{13}CO CP/MAS NMR spectrum of $(NMe_4)_2[H_2Ni_{12}(CO)_{21}] \cdot 2THF$ in the carbonyl region consists of five distinct resonances compared to four resonances found in solution. In order to confirm this, ^{13}C CP/MAS spectra (Fig. 3) of $(NMe_4)_2[H_2Ni_{12}(CO)_{21}]$ (45% ^{13}CO enrichment) were measured. Comparison of the solid state ^{13}CO chemical shifts in Fig. 3 with those found in solution [8] (see Table 4), allows the three resonances at 189.3, 198.2 and 223.7 ppm to be readily assigned to the terminal carbonyls on the inner (T_i) and outer (T_o) layers and the bridging carbonyls on the outer (B_o) layer, respectively. However, in the solid state, there are two resonances due to the bridging carbonyls on the inner layer (B_i) at 238.5 and 246.4 ppm compared to a single resonance in solution [8] (see Table 4). It is reasonable to assume that the B_i carbonyls experience similar $^1H-^{13}C$ cross polarisation through dipolar interactions and, since this is proportional to $d(C...H)^{-3}$, this interaction is more efficient within the anion than between the cation/anion or anion/solvent of crystallisation. Furthermore, the two resonances at 238.5 and 246.4 ppm have similar side band patterns as a result of similar chemical shift anisotropies and therefore their relative intensities are ca. 2:4, respectively (see Fig. 3). Their assignment then follows from a consideration of the X-ray structure of $(NMe_4)_2[H_2Ni_{12}(CO)_{21}]$ (see Fig. 1). Thus, two of the B_i carbonyls are displaced downwards from the central Ni_6 plane (C2 and C2*) and four of the B_i carbonyls are displaced upwards (C1, C1* C3 and C3*) which are assigned to the resonances at 238.5 and 246.4 ppm, respectively. The absence of a shoulder on the resonance at 238.5 ppm is also consistent with this assignment since this resonance is due only to C2 and C2*; the other resonances usually have shoulders due to the presence of more than one type of symmetry-related carbonyl group (e.g. the resonance due to B_o at 223.7 ppm is due to C6, C6*, C9, C11, C11* and C13). It is surprising, however, that only the chemical shifts for the different B_i carbonyls are signifi-

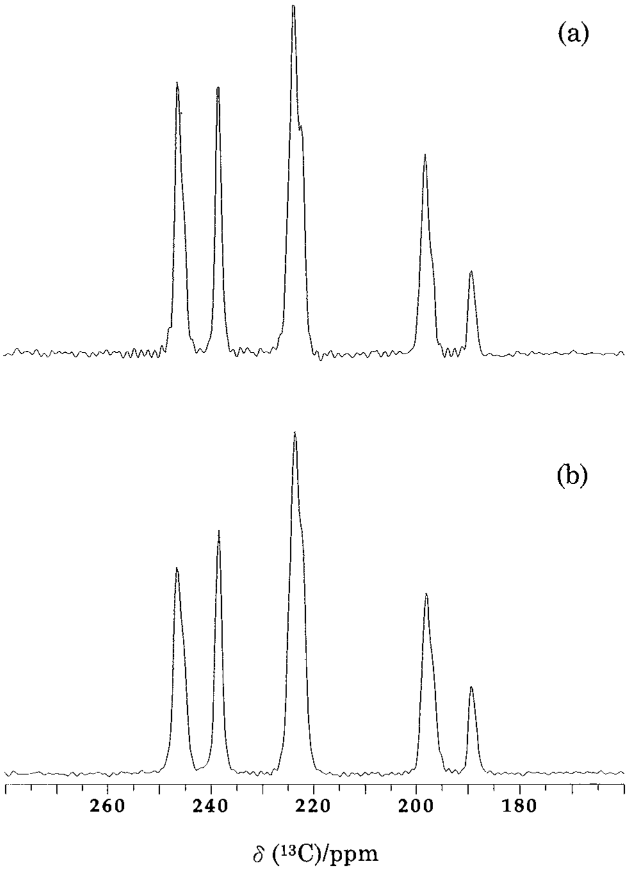

Fig. 3. ^{13}CO region of the CP/MAS NMR spectra of $(NMe_4)_2[H_2Ni_{12}(CO)_{21}] \cdot 2THF$ (45% ^{13}CO). (a) 344 K, (b) 297 K.

Table 4
Solid state and solution ^{13}CO and ^{1}H chemical shifts for $(NMe_4)_{4-x}$–$[H_xNi_{12}(CO)_{21}]$ ($x = 1$ and 2)

	$[H_2Ni_{12}(CO)_{21}]^{2-}$		$[HNi_{12}(CO)_{21}]^{3-}$	
^{13}C	Solid[a]	Solution[b]	Solid[c]	Solution[d]
T_i	189.3	189.3	190.6, 192.0 (sh)	190.5
T_o	198.2	196.0	196.9, 198.2 (sh)	196.8
B_o	223.7	219.3	226.1 (sh), 230.6	228.1
B_i	238.5, 246.4	239.9	238.6, 246.0, 249.5, 253.8	248.1
^{1}H	−18.3, −19.3	−18.3	−25.8	−24.2

[a] Room temperature, [b] 198 K [8], [c] 231 K, [d] 193 K [8].

cantly different whereas the inequivalent carbonyls in each of the T_o, T_i and B_o groups have rather similar chemical shift values.

The r.t. solid state ^{1}H MAS NMR spectrum of $(NMe_4)_2[H_2Ni_{12}(CO)_{21}] \cdot 2THF$ (Fig. 4b) consists of a very intense resonance (3.2 ppm) due to the methyl groups, which submerges the resonances due to the solvent of crystallisation, and two weaker resonances due to the hydrides at −18.3 and −19.3 ppm; this spectrum is unchanged at 205 K. However, the two hydride resonances merge into one at 340 K (Fig. 4a). It is worthwhile noting that we could not observe the hydride resonance in $[H_2Ni_{12}(CO)_{21}]^{2-}$ when using the salts of PPN^+ or $TMBA^+$ due to the overlapping cation resonances and, although it was possible to observe the hydride resonance in $(NEt_4)_2[H_2Ni_{12}(CO)_{21}]$, [1] the quality of the hydride resonance was not as good as observed for the $(NMe_4)^+$ salt.

The presence of two hydride resonances in $(NMe_4)_2[H_2Ni_{12}(CO)_{21}] \cdot 2THF$ at r.t. (see Fig. 4b) is entirely consistent with the presence of a hydride in the upper and lower octahedral cavity. Since there is no change in these hydride resonances on cooling the sample to 205 K, there is no H-movement within the Ni_{12} skeleton from low to r.t. and it is probable that they are in interstitial octahedral sites on the mirror plane at temperatures of ≤ 298 K; a more complicated high field ^{1}H resonance would have been expected if the two hydrides occupied sites off the mirror plane. On heating the sample to 340 K, however, peak coalescence takes place as shown in (Fig. 4a). This is probably due to motion of each hydride within each Ni_6-octahedron about the mirror plane because the corresponding ^{13}C spectra (Fig. 3) did not provide any evidence for oscillation of the B_i carbonyls, which would also allow the two hydrides to become equivalent without any H-movement. The high field value of $\delta(^{1}H)$ is entirely consistent [1] with the H-site occupancy being displaced from the centre of the Ni_6-octahedron towards the central Ni_3-plane as found by neutron diffraction for the PPh_4^+ salt [3], (average d(Ni_o–H) 2.00, d(Ni_i–H) 1.84 Å).

The X-ray structure of $(NMe_4)_3[HNi_{12}(CO)_{21}] \cdot Me_2CO$ shows that all the carbonyls are inequivalent and, as a result, the solid state ^{13}CO CP/MAS NMR spectrum with high power ^{1}H-decoupling at 231 K (Fig. 5b) is much more complicated. As found for $(NMe_4)_2[H_2Ni_{12}(CO)_{21}]$, the largest difference between the values of δ(CO) in solution and the solid state are associated with the B_i carbonyls and analysis of the X-ray data for $(NMe_4)_3[HNi_{12}(CO)_{21}]$ shows that the symmetry of the inner bridging carbonyls with respect to the central Ni_6-plane is quite different in the mono- and di-hydride structures. Thus, for $(NMe_4)_3[HNi_{12}(CO)_{21}]$ three bridging CO's (C7, C8

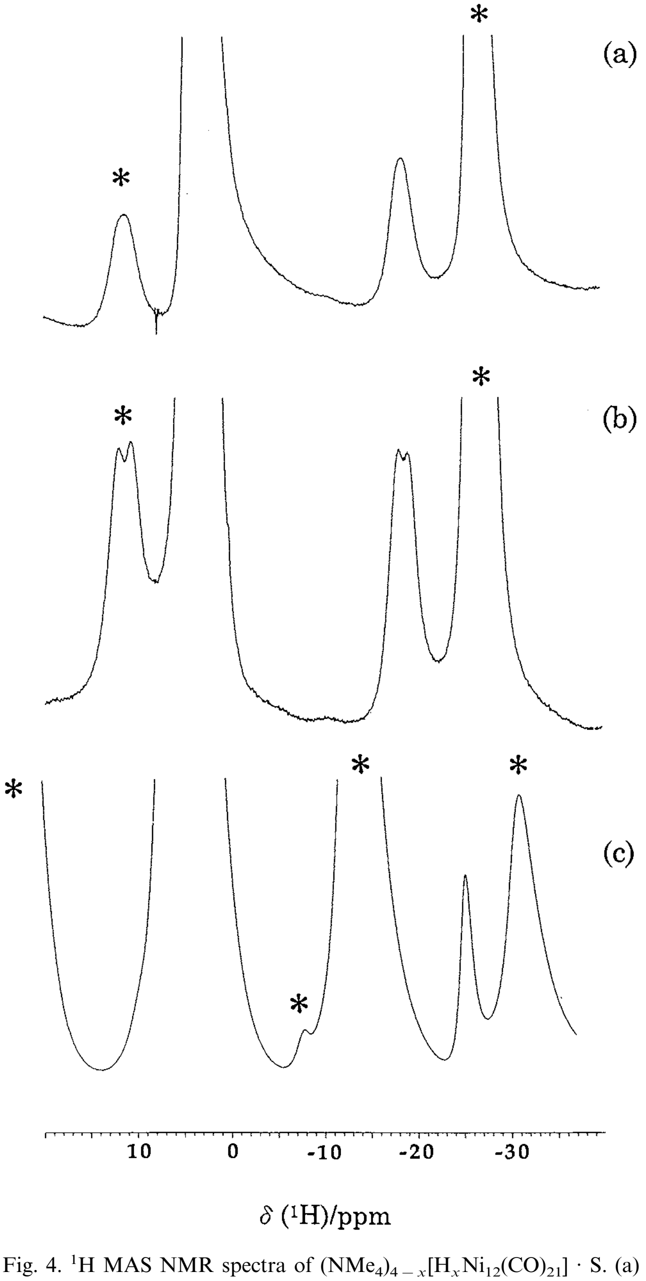

Fig. 4. ^{1}H MAS NMR spectra of $(NMe_4)_{4-x}[H_xNi_{12}(CO)_{21}] \cdot S$. (a) $x = 2$, S = 2THF, 340 K, (b) $x = 2$, S = 2THF, 297 K, (c) $x = 1$, S = Me_2CO, 190 K. * are spinning side-bands.

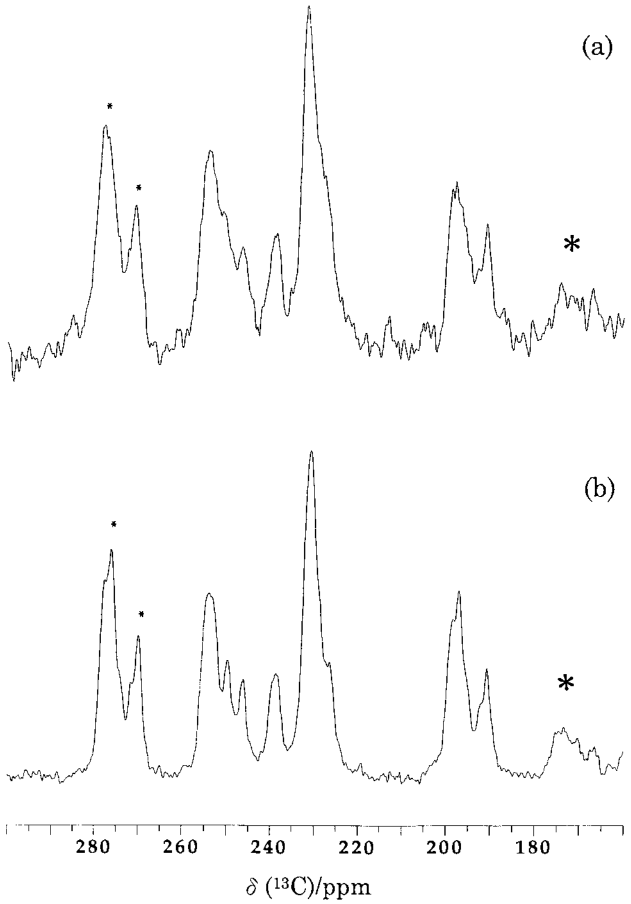

Fig. 5. ^{13}CO region of the CP/MAS NMR spectra of $(NMe_4)_3[HNi_{12}(CO)_{21}] \cdot Me_2CO$ (45% ^{13}CO). (a) 297 K, (b) 231 K. * are spinning side-bands.

and C9) are almost coplanar with the central Ni_6-plane, C6 is bent towards the hydride and the other two CO's (C4 and C5) are in intermediate positions, vide supra. Using similar reasoning for the assignment of the resonances due to the B_i carbonyls in $(NMe_4)_2[H_2Ni_{12}(CO)_{21}]$, vide supra, it is reasonable to assign the four lowest field resonances to C6, 238.6; C5, 246.0; C4, 249.5; C7, C8, C9, 253.8 ppm and this assignment is supported by the fact that this gives an average value of 249.3 ppm which is comparable to that found in solution (see Table 4).

Each of the other three main resonances due to T_i, T_o and B_o has a shoulder (Fig. 5b). Since the T_o and B_o carbonyls on the half of the Ni_{12} cluster containing the hydride will experience additional $^1H-^{13}CO$ cross polarisation from the hydride, it is reasonable to make the following assignments, T_o: C16, C17, C18, 196.9; C10, C11, C12, 198.2; B_o: C13, C14, C15, 226.1; C19, C20, C21, 230.6 ppm. Assignment of the T_i resonances is less straightforward but it should be noted that C1 and C3 are distorted downward from the Ni6-plane whereas C3 is distorted in the opposite direction[6]; this could allow the more intense resonance at 190.6 ppm to be assigned to C1 and C2 with the shoulder at 192 ppm being due to C3.

Increasing the temperature from 231 to 298 K (Fig. 5) results in a broadening of the ^{13}CO resonances with a concomitant decrease in S:N. This suggests that, in this case, there is some carbonyl movement but variable temperature ^{1}H MAS NMR spectra suggest little or no H-movement, vide infra.

The solid state ^{1}H-NMR spectrum of $(NMe_4)_3[HNi_{12}(CO)_{21}]$ at 190 K (Fig. 4c) consists of a single hydride resonance at −25.8 ppm and the chemical shift and line-width are invariant with temperature (190–340 K). The higher field chemical shift of the hydride in the mono- versus the di-hydride is consistent with a larger displacement of the hydride away from the centre of the metal octahedron [1]; this is in keeping with the H-displacement towards the central Ni_3-plane (Ni_i) found in the neutron diffraction studies on $(PPh_4)_2[H_2Ni_{12}(CO)_{21}]$ [3] (average d(Ni_i–H) 1.845, d(Ni_o–H) 2.00 Å) and $(AsPh_4)_3[HNi_{12}(CO)_{21}]$ [3] (average d(Ni_i–H) 1.72, d(Ni_o–H) 2.22 Å). Furthermore, although it has been suggested that H-oscillation between the two octahedral cavities may occur in solution [8], the lack of variation in δ(H) with temperature for the mono-hydride cluster in the solid state suggests there is little H-movement in this case.

4. Experimental section

4.1. General

The $[NMe_4]_3[HNi_{12}(CO)_{21}]$ and $[NMe_4]_2[H_2Ni_{12}(CO)_{21}]$ salts, as well as their ^{13}CO enriched congeners, were synthesised by literature methods [8,9]. NMR: Bruker MSL-200 (200 MHz for ^{1}H, 50.3 MHz for ^{13}C) and DSX-200. CP/MAS or MAS with a high power ^{1}H-decoupling pulse sequence was used to observe ^{13}C spectra. The MAS rate was 4–6 kHz.

X-ray quality crystals of both $[NMe_4]_3[HNi_{12}(CO)_{21}] \cdot Me_2CO$ and $[NMe_4]_2[H_2Ni_{12}(CO)_{21}] \cdot 2THF$ were obtained by layering acetone and THF solutions, respectively with di-isopropyl alcohol under a nitrogen atmosphere.

4.2. X-ray structure determinations

X-ray data was collected on a Rigaku AFC6S diffractometer equipped with Mo–K_α radiation (λ = 0.71073 Å) and a graphite monochromator. Selected

---

[6] Further details of the crystallographic structure investigaton can be obtained from the Director of the Cambridge Crystallographic Data Centre, 12 Union Road, Cambridge CB2 1EZ, UK on quoting the full journal citation.

Table 5
Crystal data and structure refinement for $(NMe_4)_3[HNi_{12}(CO)_{21}] \cdot Me_2CO$ and $(NMe_4)_2[H_2Ni_{12}(CO)_{21}] \cdot 2THF$

	$(NMe_4)_3$ $[HNi_{12}(CO)_{21}]$ $\cdot Me_2CO$	$(NMe_4)_2$ $[H_2Ni_{12}(CO)_{21}]$ $\cdot 2THF$
Empirical formula	$C_{36}H_{43}N_3Ni_{12}O_{22}$	$C_{37}H_{42}N_2Ni_{12}O_{23}$
Formula weight	1574.25	1587.25
Crystal size (mm)	0.30 × 0.25 × 0.10	0.60 × 0.15 × 0.10
Crystal system	Monoclinic	Orthorhombic
Space group	$P2_1/c$	*Pnma*
a (Å)	13.472(7)	24.243(13)
b (Å)	15.791(8)	22.106(8)
c (Å)	24.850(13)	9.716(16)
α (°)	90	90
β (°)	98.05(5)	90
γ (°)	90	90
V (Å^3)	5234(5)	5154(9)
Z	4	4
$D_{calc.}$ (g cm^{-3})	1.998	2.046
μ (Mo–K$_\alpha$) (mm^{-1})	4.284	4.352
Temperature (K)	153(2)	153(2)
λ (Å)	0.71073	0.71073
Scan technique	ϖ	ϖ
Reflections collected	6886	3448
Independent reflections	6544	3448
Reflections observed ($I > 2\sigma(I)$)	4801	1902
2θ-range	5–45	5–45
Absorption correction	Semi-empirical with ψ-scans	
Min./max. transmission	0.429/1.000	0.936/1.000
R_1 ($I > 2\sigma(I)$)	0.041	0.056
wR_2 (all data)	0.100	0.169
Max. diff. peak/hole (e Å^{-3})	0.693/−0.666	0.724/−0.773

crystals were mounted on glass fibres following oil immersion and held at −120°C. The structures were solved by direct methods and full matrix least-squares refinement on F^2 using all data, was carried out with the SHELX 97 program [10]. All non-hydrogen atoms were refined anisotropically (except for the THF molecule in $[NMe_4]_2[H_2Ni_{12}(CO)_{21}] \cdot 2THF$, methyl groups and the acetone molecule in $[NMe_4]_3[HNi_{12}(CO)_{21}] \cdot Me_2CO$, in which the C and O atoms were refined isotropically) and hydrogen atoms were included in the calculated positions ($d(C–H) = 0.95$ Å). Crystallographic details for both structures are shown in Table 5.

Acknowledgements

We thank the EC (Contract No. CHRX-CT93-0277), Monbusho Grant-in-aid (No. 09640606), the Japan Society for the Promotion of Science for financial support and the Royal Society and British Council for tavel funds. B.T. Heaton also thanks the Nuffield Foundation for the award of a Research Fellowship.

References

[1] (a) T. Eguchi, B.T. Heaton, R. Harding, et al., J. Chem. Soc. Dalton Trans. (1996) 625. (b) R.A. Harding, H. Nakayama, T. Eguchi, B.T. Heaton, N. Nakamura, A.K. Smith, Polyhedron (1998) accepted for publication.
[2] T. Eguchi, R.A. Harding, B.T. Heaton, et al., J. Chem. Soc. Dalton Trans. (1997) 479.
[3] R.W. Broach, Ph.D Thesis, University of Wisconsin, Madison, Wisconsin, (1977).
[4] P. Chini, G. Longoni, M. Manassero, M. Sansoni, VII Cong. Ass. Ital. Crist. Ferrara Commun. 34 (1977) 85.
[5] R.W. Broach, L.F. Dahl, G. Longoni, P. Chini, A.J. Schultz, J.M. Williams, ACS Adv. Chem. Ser. 167 (1978) 93.
[6] A.F. Masters, J.T. Meyer, Polyhedron 14 (1995) 339.
[7] P.L. Stanghellini, G. Longoni, J. Chem. Soc. Dalton Trans. (1987) 685.
[8] G. Longoni, B.T. Heaton, P. Chini, J. Chem. Soc. Dalton Trans. (1980) 1537.
[9] A. Ceriotti, P. Chini, R. Della Pergola, G. Longoni, Inorg. Chem. 22 (1983) 1595.
[10] G.M. Sheldrick, SHELX 97, Structure evaluation program, Götingen (1997).